

These results show that CNT/FE and CNT/FE-OBD possess much higher hardness compared to OBD-aged and unaged CB/FE and FE. Therefore, the OBD resistance of this nanocomposite is higher compared to others. Data in Table 2 also show that FE-OBD and CNT/FE-OBD have lower hardness compared to FE and CNT/FE, respectively, while CB/FE-OBD and CB/FE have the same hardness. However, the changes in hardness of FE due to OBD test are bigger than the others. CB/FE-OBD and CB/FE have the same hardness and probably this is due to having negative swelling of this elastomer in OBD. Normally, it is expected that negative swelling cause the increase in hardness. Again, NORSOK M-710 [17] or ISO 23926-2 [18] defines the hardness change of elastomer for most of oil field applications. Per these standards the change in hardness out the range of +10/-20 units is not acceptable. Therefore, according to Table 2 all of elastomers under study had the acceptable hardness changes oil field applications, however, as mentioned before, only CNT/FE could pass the swelling and appearance test for oil field applications.

Table 2. Hardness changes of filled and unfilled FE due to OBD test

Sample	H Shore A	ΔH Shore A
FE	59	
FE-OBD	56	-3
CB/FE	69	
CB/FE-OBD	69	0
CNT/FE	78	
CNT/FE-OBD	76	-2

Tensile properties

In addition, the higher modulus/hardness of CNT/FE compared to CB/FE and FE should be another explanation for the results on surface, volume swelling or others after aging in OBD which were verified by us in another study [23]. This was only the part of a project that covers both characterization and physical/mechanical experiments. In a summary of our other study [23] on mechanical properties of filled and unfilled FE subjected to aging test in oil-based drilling fluids it was mentioned: tensile results showed that elongation at break (*EB*) and tensile strength (*TS*) of FE and CB/FE were decreased considerably due to OBD aging. However, for CNT/FE, those parameters had slight changes. Normal modulus (*NM*) of all samples under study at low strains had negligible changes after OBD aging. The order of tensile properties for OBD-aged samples was: CNT/FE-OBD > CB/FE-OBD > FE-OBD. In another previous study, also we verified mechanical properties of original elastomers [24] and the summary was as follows: under the same conditions, the order of *EB* was FE > CB/FE > CNT/FE. *NM* at the same conditions was in the order of CNT/FE > CB/FE > FE. *TS* had the order of CNT/FE > CB/FE > FE.

CNTs have three especially important properties: mechanical, thermal and electronic ones. Most of the results such as swelling, thermal stability and degradation in this paper could be explained from mechanical properties of CNTs. This is the main role for CNTs in most of polymer composites.

Low swelling and weight changes during aging of CNT/FE could be explained by the high hardness or modulus of the composites containing CNT, which could resist the swelling during aging and also lead to less weight changes.

Thermal stability and degradation during aging of CNT/FE can also be explained as follows: CNT composite higher modulus and a network of high modulus CNT lead to denser polymer chain packing. Thus, the diffusivity of the chemicals of the drilling fluid to the nanocomposite can be reduced and lead to increase in the thermal stability and reduce degradation rate of nanocomposite.

Verifying resistance of filled and unfilled FE to OBD

Sugama *et al.* [25] evaluated the degradation of O-rings made with different types of elastomers including FE in 300 °C steam, heat, and chemically aggressive environments (drilling and geo-brine fluids). The assessed factors included the extent of oxidation, microdefects, permeation of ionic species from the test environments into the O-rings, and silicate-related scale-deposition. According to their results FE performed poorly in all but high heat environments. Reactions between calcium and degradation derivatives caused calcium permeation into the elastomer body (a depth of at least 0.4 mm from the surface), resulting in the material hardening at the edges. The drilling and geo-brine fluids visibly damaged FE O-rings and the morphological image revealed a rim-like layer at the subsurface. Additionally, microcracks were observed in the interfacial regions between the rim layer and the rest of the O-ring body, demonstrating that the formation of this rim was resulted in structural damage. These data, in conjunction with previous studies [26–32], suggested that the poly-VDF was the first to be degraded in the structure of the tested FE. Formation of calcium salts (possibly calcium fluoride) could have contributed to the O-ring-edge hardening in the drilling and geo-brine fluids.

In our drilling mud, there was Ca, therefore, in our FE-OBD and CB/FE-OBD the same phenomenon (the O-ring-edge hardening with calcium in the drilling fluids) would happen and cause cracks and degradation of the surface. However, CNT/FE-OBD could resist OBD test. Furthermore, this nanocomposite had barrier properties toward the permeation of Ca into the nanocomposite as would be explained subsequently. The Ca degradation products were evaluated by XRD and will be discussed at the end of paper.

Degradation of FE in mud with amine species normally was a nucleophilic substitution with addition of amine

and then removal of fluorine, formation of a double bond, and then further degradation [33].

Pham *et al.* [34] for the thermal stability of the CNT/FE reasoned that the interactions between CNT and FE resulted in increased physical and chemical cross-linking points which prevented the degradation of the polymer chains. Furthermore, in comparison with CB, CNTs showed higher reinforcing efficiency due to their higher aspect ratio and surface area that resulted in higher cross-link density and stronger filler–polymer interaction [35]. Moreover, Endo *et al.* [1] reasoned that thermal stability of FE near CNT was due to the presence of bounded rubber to CNT and concluded that this structure could prevent the decomposition of rubber at high temperatures by resisting the molecular mobility. The same reasons as mentioned above could help in explanation of the increased resistance to OBD and temperatures of CNT/FE. The barrier property of composites relied on the geometry of the filler (property, size, shape, concentration, and orientation), matrix, temperature, interaction between the filler and the matrix, *etc.* [36, 37].

Wei *et al.* [38] reported that reduction in permeability of GO/FKM (GO – graphene oxide, FKM – enhanced fluoroelastomer) to organic solvent (such as methyl ethyl ketone) indicated the improved liquid barrier properties. The diffusion depended on the concentration of free space available in the matrix which accommodated the penetration of solvent molecule [39, 40]. The addition of the GO and RGO (reduced graphene oxide) reduced the available free space and restricted segmental mobility of the rubber matrix.

The nanocomposites exhibit similar barrier properties toward the Ca when Ca penetrates into nanocomposites from OBD. Due to this reason and other reasons mentioned previously for induced stability of FE by CNT, the surface of CNT/FE-OBD is not degraded due to OBD test and this nanocomposite could resist the OBD at high temperature and pressure. CNT has also anti-oxidation effect (belonging to electronic chemical properties of CNT), therefore, caused reduction of degradation rate [34]. In one of our previous publications [41] we proved that our CNT-filled FE obeyed thin film behavior meaning that the surface area of 8 % CNT was so big that the distance between two adjacent CNT in FE was less than 100 nm (thin film). We also observed by FESEM (Field Emission Scanning Electron Microscope) that the distance between each two adjacent CNT was less than 100 nm and therefore there was a large amount of the rubber near to CNT and in fact most of the rubber was near to CNT (our CNT dimensions: outside diameter > 50 nm and length of 10–20 μm). We also proved with different techniques (*e.g.* DMA, Dynamic Mechanical Analysis) that there was a large amount of bound rubber and affected different properties like tensile properties. Those were due to high aspect ratio and high surface area of CNT. Obeying thin film behavior and having large amount of bound rubber could result in high barrier properties of CNT/FE to OBD and also CNT/FE resistance to OBD.

XRD analyses

To confirm the conclusions mentioned in the previous section the XRD analyses were performed for filled and unfilled FE-OBD samples. Figure 10 shows the XRD spectra of these samples. There was CaCl_2 in our OBD and due to the chemical degradation, it could undergo reaction to produce CaF_2 . According to Pandurangappa and Lakshminarasappa [42] researches, XRD spectra of CaF_2 showed sharp peaks around $2\theta = 28.5^\circ, 47.0^\circ, 56.5^\circ, 69.0^\circ, 76.5^\circ$ and 88.5° . Furthermore, CaCl_2 showed sharp peaks in XRD spectra at $2\theta = 31.7^\circ$ [43], $13.5^\circ, 14.0^\circ, 14.5^\circ, 15.0^\circ, 15.5^\circ, 17.5^\circ, 20.5^\circ, 21.5^\circ, 22.0^\circ, 23.0^\circ, 24.5^\circ, 26.0^\circ, 26.5^\circ, 31.0^\circ, 33.0^\circ, 34.0^\circ, 35.0^\circ$ [44], $38.2^\circ, 39.2^\circ, 50.6^\circ$ and 56.4° [45]. Our previous publication on XRD results [23, 24] showed that VDF segments of FE, CB/FE and CNT/FE were crystalline and the crystals were in the form of γ -phase with the following peaks: $2\theta = 28.17^\circ, 36.08^\circ, 39.26^\circ, 39.35^\circ, 39.47^\circ, 41.05^\circ, 42.12^\circ, 43.16^\circ, 46.66^\circ, 54.43^\circ$ and 55.52° . Furthermore, TFE segments were also crystalline with peaks at $2\theta = 31.8^\circ, 36.3^\circ, 41.7^\circ, 50.3^\circ, 56.6^\circ, 66.4^\circ$ and 69.2° [23, 24]. It is noticeable that all of peaks presented in Fig. 10 can be assigned with above mentioned peaks. If the peaks positions are of the γ -phase, TFE segments and CaF_2 in comparison with those of CaCl_2 show that some of CaCl_2 peaks are overlapped with others peaks. However, for CaCl_2 the peaks at $31.0^\circ, 33.0^\circ, 34.0^\circ$ and 35.0° are not overlapped and they could be used to show the presence or absence of CaCl_2 and also its XRD emission intensity. Furthermore, the same things could be mentioned for CaF_2 and the peaks at $45\text{--}46^\circ$ also only belong to CaF_2 , CaClF and other complexes of Ca which are not overlapped with any other peak. Therefore, this peak could be used to show the presence and absence of CaF_2 and also its XRD emission intensity.

Figure 10 shows that the XRD peaks of CaF_2 which are mentioned above have higher intensity and surface area in cases of FE-OBD and CB/FE-OBD compared to those of CNT/FE-OBD. However, the same figure shows that the XRD peaks of CaCl_2 which also are mentioned above have higher intensity and surface area in case of CNT/FE-OBD

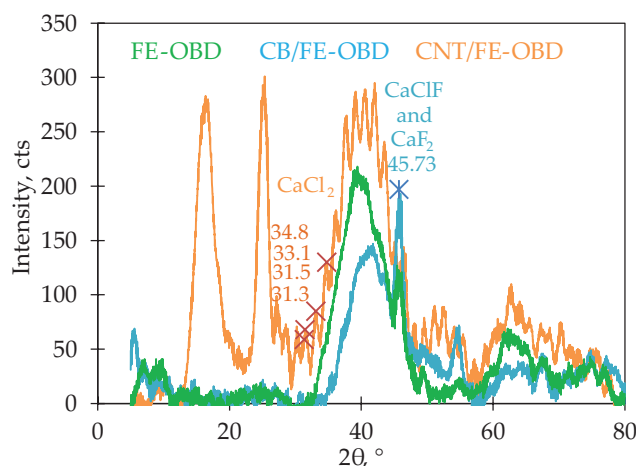


Fig. 10. XRD spectra of overlaid filled and unfilled FE-OBD

Table 3. XRD peak list of FE-OBD, CB/FE-OBD and CNT/FE-OBD

FE-OBD		CB/FE-OBD		CNT/FE-OBD	
2 θ , °	Intensity, cts	2 θ , °	Intensity, cts	2 θ , °	Intensity, cts
6.77	31.80	5.52	63.55	6.26	2.45
10.07	26.37	7.42	28.08	8.79	11.19
12.72	7.35	9.14	21.84	10.83	14.74
14.96	6.69	10.85	13.57	15.38	223.72
16.78	7.81	12.70	9.26	16.84	263.76
20.72	3.46	14.46	13.36	25.31	287.85
23.65	11.23	17.69	6.33	28.78	64.47
25.33	10.84	22.72	9.52	30.11	53.61
27.06	9.86	24.80	11.34	31.62	62.62
33.91	39.63	26.85	10.64	33.08	78.77
39.11	207.17	28.65	4.17	34.57	122.87
43.70	123.25	30.62	5.35	37.67	261.03
45.93	113.47	36.79	51.05	39.12	278.49
49.58	27.00	39.20	117.25	42.14	281.27
54.66	19.36	42.00	137.23	43.55	236.16
62.16	62.95	45.65	176.77	46.61	135.30
67.75	37.37	54.82	62.69	48.06	65.81
71.52	31.20	62.13	29.88	49.58	71.37
75.07	36.93	64.63	31.38	51.08	85.57
77.08	28.08	67.48	38.75	52.60	83.65
		70.83	24.20	55.60	57.47
		74.80	42.77	57.10	32.01
		77.08	37.30	58.65	43.70
				62.42	97.27
				65.65	73.45
				67.27	67.97
				70.35	68.33
				76.03	41.56
				78.03	16.73

compared to those of FE-OBD and CB/FE-OBD, particularly the peaks at 31.0°, 33.0°, 34.0° and 35.0°. In CNT/FE-OBD the CaF₂ and CaClF peaks are not appeared, therefore, the intensity of them is zero but CaCl₂ peaks appeared. Also in FE-OBD and CB/FE-OBD the CaCl₂ peaks do not appeared while CaF₂ and CaClF peaks do. Therefore, for comparing peak intensity of CaF₂ and CaClF in elastomers there is no need of any reference peaks for data normalization because the peak intensities for each of these chemicals in one elastomer are zero whereas the same chemical have peak intensity greater than zero in the other elastomer. These could be seen in Table 3 which shows XRD peak list of FE-OBD, CB/FE-OBD and CNT/FE-OBD.

Therefore, it could be concluded that FE-OBD and CB/FE-OBD had higher CaF₂ content while CNT/FE-OBD had higher CaCl₂ content. According to Rehmer *et al.* [46] researches, by the reaction of CaCl₂ with HF, the products would be CaF₂ and CaClF. In our elastomers, HF liberated from the fluororubber particularly during OBD test

which run at high temperature and OBD contained amine species [29, 47]. Rehmer *et al.* [46] reported XRD spectrum of CaF₂ and CaClF that showed the main peaks of these two chemicals, particularly the spectrum contained three peaks with 2 θ = 46–47° which belonged to CaF₂ and CaClF. In Fig. 10 these peaks have higher intensity in the case of FE-OBD and CB/FE-OBD comparing to those of CNT/FE-OBD.

This indicated that FE-OBD and CB/FE-OBD have higher concentration of CaF₂ and CaClF compared to CNT/FE-OBD. As a result, it was concluded that during OBD aging tests of FE-OBD and CB/FE-OBD, reaction between Ca and degradation derivatives caused Ca permeation into the elastomer body. Then, CaCl₂ reacted with rubber degradation products and CaF₂, CaClF and other Ca complexes were produced. This phenomenon resulted in the material hardening at the edges in the OBD aging test and caused cracks and degradation of the surfaces of FE-OBD and CB/FE-OBD. However, in the case of

CNT/FE-OBD this phenomenon did not happen and the CaCl_2 did not react and remained unchanged. Therefore, the O-ring-edge hardening did not happen and CNT/FE-OBD was resistant to OBD. The reasons for this OBD resistance were explained in the previous section.

The produced CaF_2 and CaClF affect the roughness and other AFM parameters of FE-OBD and CB/FE-OBD. Ghosh and De [47] reported that the fluororubber exhibited comparatively smooth surface except for the randomly distributed particles protruding from the matrix [47]. Those particles were unreacted $\text{Ca}(\text{OH})_2$ and CaF_2 produced during vulcanization by reaction of $\text{Ca}(\text{OH})_2$ with HF liberated from the fluororubber.

As mentioned before CNT/FE-OBD was resistant to OBD therefore CNT/FE can be applied as sealing rubbers (for example O-rings) in OBD drilling for oil and gas. In contrast, original FE compound and CB/FE are not resistant to OBD, therefore, FE or CB/FE cannot be applied as the above mentioned sealing rubbers.

CONCLUSIONS

The high temperature and pressure OBD resistance of the CNT/FE *vis-à-vis* CB/FE and FE were assessed by AFM, weight gain, swelling test, and also optical microscopy and XRD. All of the above mentioned test results showed that while original unfilled rubber (FE) was not resistant to the OBD, introduction of CNT into FE induced resistance of FE to OBD. Also CB did not induce resistance of FE to OBD.

AFM results showed that surface of FE-OBD degraded and changed considerably compared to that of FE. The similar results were observed when CB/FE-OBD surface was compared to CB/FE. However, the surface of CNT/FE-OBD was the same as that of original compound of CNT/FE.

The other test results showed that the surface of CNT/FE-OBD was not degraded and free of defects. However, for FE and CB/FE the surface was full of defects. Weight gain and swelling test also showed the chemical degradation of FE and CB/FE in OBD while CNT/FE was resistant to OBD.

Optical microscopy images also showed that FE-OBD and CB/FE-OBD surfaces degraded and were full of cracks but that of CNT/FE-OBD was not degraded and had no cracks. The hardness test results also showed that the change in hardness of CNT/FE-OBD compared to CNT/FE was negligible and indicated that the degradation was negligible. XRD results showed that when FE and CB/FE were contacted with aggressive fluids containing calcium, reactions between calcium and degradation derivatives caused calcium permeation into the elastomer body and resulted in the material hardening at the edges and caused cracks and degradation of the surfaces. However, reactions between calcium and degradation derivatives and the following material edge hardening did not happen for CNT/FE-OBD and it was resistant to OBD.

The final conclusion is that CNT/FE is suitable for using as sealing rubbers (for example O-rings) in OBD

drilling for oil and gas. In contrast original FE compound without CNT or FE with CB can not be used as the above mentioned sealing rubbers.

ACKNOWLEDGMENTS

We thank the Schlumberger WTA Malaysia Sdn Bhd and also Engineers Ling Kong Teng and Daniel Thomas Melice from this company for advice and help with this study and also running drilling fluid aging tests.

REFERENCES

- [1] Endo M., Noguchi T., Ito M. *et al.*: *Advanced Functional Materials* **2008**, 18, 3403.
<http://dx.doi.org/10.1002/adfm.200801136>
- [2] *Pat. US* 8 901 228 (2014).
- [3] Ito M., Noguchi T., Ueki H. *et al.*: *Materials Research Bulletin* **2011**, 46, 1480.
<http://dx.doi.org/10.1016/j.materresbull.2011.04.028>
- [4] Zhong A.: "Residual Stress, Thermomechanics & Infrared Imaging, Hybrid Techniques and Inverse Problems", Proceedings of the 2016 Annual Conference on Experimental and Applied Mechanics, Springer, Germany **2016**, 9, 65.
- [5] *Pat. Appl. US* 0 154 454 (2014).
- [6] Molavi F.K., Soltani S., Naderi G., Bagheri R.: *Polyolefins Journal* **2016**, 3, 69.
<http://dx.doi.org/10.22063/poj.2016.1293>
- [7] Maiti M., Bhowmick A.K.: *Polymer* **2006**, 47, 6156.
<http://dx.doi.org/10.1016/j.polymer.2006.06.032>
- [8] Morozov I.A., Solodko V.N., Kurakin A.Y.: *Polymer Testing* **2015**, 44, 197.
<http://dx.doi.org/10.1016/j.polymertesting.2015.04.007>
- [9] Mishra S., Shimpi N.G., Mali A.D.: *Journal of Polymer Research* **2011**, 18, 1715.
<http://dx.doi.org/10.1007/s10965-011-9577-7>
- [10] Bhattacharyya S., Sinturel C., Bahloul O. *et al.*: *Carbon* **2008**, 46, 1037.
<http://dx.doi.org/10.1016/j.carbon.2008.03.011>
- [11] Gabriel D., Karbach A., Drechsler D. *et al.*: *Colloid and Polymer Science* **2016**, 294, 501.
<http://dx.doi.org/10.1007/s00396-015-3802-6>
- [12] Javadi S., Sadroddini M., Razzaghi-Kashani M. *et al.*: *Journal of Polymer Research* **2015**, 22, 1.
<http://dx.doi.org/10.1007/s10965-015-0805-4>
- [13] Wang D., Fujinami S., Nakajima K. *et al.*: *Polymer* **2010**, 51, 2455.
<http://dx.doi.org/10.1016/j.polymer.2010.03.052>
- [14] Kummali M.M., Miccio L.A., Schwartz G.A. *et al.*: *Polymer* **2013**, 54, 4980.
<http://dx.doi.org/10.1016/j.polymer.2013.07.032>
- [15] [https://www.xiameter.com/en/ExploreSilicones/Documents/45-0113E-01_Fluid_new2_\(3\).pdf](https://www.xiameter.com/en/ExploreSilicones/Documents/45-0113E-01_Fluid_new2_(3).pdf) (access date 28.05.2017).
- [16] http://www.prepol.com/Ppe-Uploads/Elastomer_guide_chemical_compatibility.pdf (access date 28.05.2017).

- [17] The NORSOK M-710: 2001. Qualification of nonmetallic sealing materials and manufacturers.
- [18] ISO 23936-2:2011(En). Petroleum, petrochemical and natural gas industries — Non-metallic materials in contact with media related to oil and gas production — Part 2: Elastomers.
- [19] Epikhin A., Ushakov A., Barztaikin V. *et al.*: "Experimental research of drilling mud influence on mud motor mechanical rubber components" IOP Conference Series: Earth and Environmental Science, IOP Publishing, 6–10 April, Tomsk, Russia 2015, p. 012051.
- [20] Kader M.A., Bhowmick A.K.: *Polymer Degradation and Stability* **2003**, 79, 283.
[http://dx.doi.org/10.1016/S0141-3910\(02\)00292-6](http://dx.doi.org/10.1016/S0141-3910(02)00292-6)
- [21] Ghari H.S., Shakouri Z., Shirazi M.M.A.: *Plastics, Rubber and Composites* **2014**, 43, 177.
<http://dx.doi.org/10.1179/1743289814Y.00000000087>
- [22] Maiti M., Bhowmick A.K.: *Journal of Applied Polymer Science* **2007**, 105, 435.
<http://dx.doi.org/10.1002/app.26052>
- [23] Heidarian J., Hassan A.: "Stable mechanical properties of carbon nanotube filled fluoroelastomers subjected to aging test in oil based drilling fluids" 2017, submitted.
- [24] Heidarian J., Hassan A.: *Polish Journal of Chemical Technology* **2017**, 19, 132.
<http://dx.doi.org/10.1515/pjct-2016-0050>
- [25] Sugama T., Pyatina T., Redline E. *et al.*: *Polymer Degradation and Stability* **2015**, 120, 328.
<http://dx.doi.org/10.1016/j.polymdegradstab.2015.07.010>
- [26] Sugama T., Sullivan B.: *Journal of Materials Science Letters* **2001**, 20, 1737.
<http://dx.doi.org/10.1023/A:1012454209899>
- [27] Harwood H.J.: *Journal of Testing and Evaluation* **1983**, 11, 289.
<http://dx.doi.org/10.1520/JTE10292J>
- [28] Mitra S., Ghanbari-Siahkali A., Kingshott P. *et al.*: *Polymer Degradation and Stability* **2004**, 83, 195.
[http://dx.doi.org/10.1016/S0141-3910\(03\)00235-0](http://dx.doi.org/10.1016/S0141-3910(03)00235-0)
- [29] Theodore A., Zinbo M., Carter R.: *Journal of Applied Polymer Science* **1996**, 61, 2065.
[http://dx.doi.org/10.1002/\(SICI\)1097-4628\(19960919\)61:12%3C2065::AID-APP3%3E-3.0.CO;2-8](http://dx.doi.org/10.1002/(SICI)1097-4628(19960919)61:12%3C2065::AID-APP3%3E-3.0.CO;2-8)
- [30] Banik I., Bhowmick A.K., Raghavan S. *et al.*: *Polymer Degradation and Stability* **1999**, 63, 413.
[http://dx.doi.org/10.1016/S0141-3910\(98\)00122-0](http://dx.doi.org/10.1016/S0141-3910(98)00122-0)
- [31] Knight G., Wright W.: *Thermochimica Acta* **1983**, 60, 187.
[http://dx.doi.org/10.1016/0040-6031\(83\)80269-X](http://dx.doi.org/10.1016/0040-6031(83)80269-X)
- [32] Ross G., Watts J., Hill M., Morrissey P.: *Polymer* **2000**, 41, 1685.
[http://dx.doi.org/10.1016/S0032-3861\(99\)00343-2](http://dx.doi.org/10.1016/S0032-3861(99)00343-2)
- [33] Benning H.G., Davidson M.: *KGK-Kautschuk Gummi Kunststoffe* **2016**, 69, 22.
- [34] Pham T.T., Sridhar V., Kim J.K.: *Polymer Composites* **2009**, 30, 121.
<http://dx.doi.org/10.1002/pc.20521>
- [35] Liu Y., Liu P., Fan Z., Duong H.: *Materials Technology: Advanced Performance Materials* **2015**, 30, 150.
<http://dx.doi.org/10.1179/17535557A15Y.0000000015>
- [36] Balachandran M., Bhagawan S.: *Journal of Polymer Research* **2012**, 19, 1.
<http://dx.doi.org/10.1007/s10965-011-9809-x>
- [37] Balachandran M., Bhagawan S.: *Journal of Applied Polymer Science* **2012**, 126, 1983.
<http://dx.doi.org/10.1002/app.36328>
- [38] Wei J., Jacob S., Qiu J.: *Composites Science and Technology* **2014**, 92, 126.
<http://dx.doi.org/10.1016/j.compscitech.2013.12.010>
- [39] Collins W.R., Lewandowski W., Schmois E. *et al.*: *Angewandte Chemie International Edition* **2011**, 50, 8848.
<http://dx.doi.org/10.1002/anie.201101371>
- [40] Stephen R., Varghese S., Joseph K. *et al.*: *Journal of Membrane Science* **2006**, 282, 162.
<http://dx.doi.org/10.1016/j.memsci.2006.05.019>
- [41] Heidarian J., Hassan A.: *Polymer Composites* **2015**, 37, 3341.
<http://dx.doi.org/10.1002/pc.23532>
- [42] Pandurangappa C., Lakshminarasappa B.N.: *Journal of Nanomedicine and Nanotechnology* **2011**, 2 (2).
<http://dx.doi.org/10.4172/2157-7439.1000108>
- [43] Chen Y., Zhao Y., Liang Z.: *Journal of Materials Chemistry A* **2015**, 3, 9137.
<http://dx.doi.org/10.1039/C5TA01198A>
- [44] Uriarte L.M., Dubessy J., Boulet P. *et al.*: *Journal of Raman Spectroscopy* **2015**, 46, 822.
<http://dx.doi.org/10.1002/jrs.4730>
- [45] Léger J.-M., Haines J., Danneels C.: *Journal of Physics and Chemistry of Solids* **1998**, 59, 1199.
[http://dx.doi.org/10.1016/S0022-3697\(98\)00057-2](http://dx.doi.org/10.1016/S0022-3697(98)00057-2)
- [46] Rehmer A., Scheurell K., Kemnitz E.: *Journal of Materials Chemistry C* **2015**, 3, 1716.
<http://dx.doi.org/10.1039/C4TC02510E>
- [47] Ghosh A., De S.: *Rubber Chemistry and Technology* **2004**, 77, 856. <http://dx.doi.org/10.5254/1.3547856>

Received 31 I 2017.